Methanol Oxidation on Stepped Pt[*n*(111) × (110)] Electrodes: A Chronoamperometric Study

T. H. M. Housmans* and M. T. M. Koper

Laboratory of Inorganic Chemistry and Catalysis, Schuit Institute of Catalysis, Eindhoven University of Technology, 5600 MB Eindhoven, The Netherlands

Received: February 4, 2003; In Final Form: May 15, 2003

The methanol oxidation reaction has been studied on Pt[*n*(111) × (110)]-type electrodes in a 0.5 M sulfuric acid and 0.025 M methanol solution, using cyclic voltammetry and chronoamperometry. The voltammetric behavior of methanol on the three electrodes under investigation [Pt(111), Pt(554), and Pt(553)] shows that the overall oxidation rate increases with an increasing step density and that the defects are affected more by the presence of methanol than terraces. The latter implies that either the decomposition products of methanol or the methanol itself preferably sit at the steps. Investigation of the chronoamperometric data showed that the steady-state current, recorded at 900 s after the start of the experiment, increases with an increasing step density. Moreover, surfaces with a higher step density display a faster dropping current, which suggests that the decomposition of methanol into CO poisoning species also preferentially takes place on the steps and defects. Unlike the stepped electrodes, most transients recorded on Pt(111) showed an initial current increase, which may be explained by the CO oxidation being faster than the methanol decomposition. This low decomposition rate is probably the result of a sufficiently low defect density and the low methanol concentration used in our experiments. Fitting the chronoamperometric data with a mathematical model, which includes the methanol decomposition reaction, the CO oxidation reaction, and the direct methanol oxidation reaction, suggests that steps and defects catalyze all these reactions. Furthermore, the model indeed predicts that when the CO oxidation rate is faster than the decomposition rate, a rising current transient can be expected, as was seen for Pt(111).

1. Introduction

From a practical and theoretical point of view, one of the most promising fuels for a fuel cell is methanol.[1−7] First, it is a liquid at room temperature and can, therefore, easily be introduced in the already existing fuel distribution system, and second, it can be produced in large quantities and is relatively safe in handling. However, from the fuel cell technology point of view, a more important consideration for choosing methanol is the fact that it can be catalytically oxidized on a platinum surface in an aqueous environment, yielding CO_2 and six electrons per methanol molecule:

$$CH_3OH + H_2O \rightarrow CO_2 + 6H^+ + 6e^- \qquad (1)$$

This reaction has a very promising thermodynamic potential of 0.04 V versus the reversible hydrogen electrode (RHE) and may, theoretically, allow for a power as high as that of a hydrogen-based fuel cell. Unfortunately, the fact that the decomposition reaction of methanol on platinum produces surface-poisoning species leads to a low catalytic activity and presents a severe inhibition for the development of the direct methanol fuel cell.

Carbon monoxide has been identified in many studies as the primary poisoning species.[1,4−6,8] The electrocatalytic oxidation of CO, both in the adsorbed and in the dissolved forms, was found to be a structure-sensitive process.[4,9,10] In a study of the role of crystalline defects on the electrocatalytic oxidation of carbon monoxide, Lebedeva et al.[11−13] showed that CO is both preferentially adsorbed and oxidized at steps and defects in the platinum electrode surface. The reaction rate constant was found to depend linearly on the fraction of steps of a (110) orientation on surfaces with a (111) terrace orientation.[12]

Like CO oxidation, the methanol decomposition on platinum has also been reported to have a pronounced structure sensitivity. Under ultrahigh-vacuum conditions, Gibson and Dubois[14] proved that the thermal decomposition of methanol is structure-sensitive by showing that a small amount of defects on the surface resulted in CO being formed at 200 K, whereas on a defect-free surface, no carbon monoxide could be detected. In a theoretical study of the methanol oxidation reaction, Desai et al.[15] showed, using density functional calculations, that defect-free Pt(111) is unreactive toward methanol decomposition to form carbon monoxide. Under electrochemical conditions, Clavilier et al.[16,17] demonstrated structure sensitivity by comparing voltammograms of the methanol oxidation reaction on the three basal planes of platinum. These experiments were later augmented by chronoamperometric, spectroscopic, and kinetic isotope studies, which all indicated a high structure sensitivity of the reaction.[18,19] Of the three basal planes of platinum, Pt(111) was found to be the least reactive toward methanol decomposition, whereas Pt(110) was found to be the most active. As a result, the surface poisoning process is slowest on Pt(111) and fastest on Pt(110). However, the Pt(111) electrode was found to give only a small initial current that degrades to an even lower level with time, whereas the Pt(110) surface deactivates much faster but remains the most efficient in oxidizing methanol.[19]

* Corresponding author. Telephone: +31-40-247-4916. Fax: +31-40-2455054. E-mail: t.h.m.housmans@tue.nl.

10.1021/jp034291k CCC: $25.00
Published on Web 07/18/2003

Despite these numerous studies, still no clarity exists on how exactly the step density influences the reaction. From an infrared study of the CO formation on step and terrace sites on a platinum electrode surface during methanol oxidation, Shin and Korzeniewski[20] concluded that methanolic CO formation is inhibited on Pt(111) at potentials in the classical hydrogen adsorption region and that the corrugated Pt(335) (a Pt[n(111) × (100)]-type electrode with $n = 4$) surface plane promotes methanol dissociative chemisorption in this potential region, thus suggesting that defects catalyze methanol decomposition. On the other hand, Tripković et al.[21] reported that the initial surface activity of methanol on stepped electrodes decreases with an increasing step density in the sequence Pt(755) > Pt(211) > Pt(311) (Pt[n(111) × (100)]-type electrodes with $n = 6$, 3, and 2, respectively), which seems contradictory to Shin and Korzeniewski's findings. In a recent article on methanol oxidation on carbon-supported platinum nanoparticles, Weaver et al.[22] suggested that to explain the observation that the methanol oxidation rate decreases with a decreasing particle size, methanol decomposition requires terrace sites rather than defect or step sites.

Given this rather unsatisfactory understanding of the influence of surface defects on methanol oxidation, our goal in this paper is to investigate the decomposition and oxidation of methanol on a series of stepped platinum single-crystal electrodes of a Pt[n(111) × (110)] orientation. Conventional techniques such as cyclic voltammetry will be used to investigate the overall electrooxidation rates of methanol on the different stepped surfaces. However, the rates of the different reaction steps will be investigated by potential step experiments and a new model, similar to models proposed by the Stuve[8,23,24] and Wieckowski groups,[25−27] will be introduced to fit the obtained chronoamperometric data and gain insight into the kinetics of the decomposition and oxidation reaction.

2. Experimental Section

A conventional electrochemical cell was cleaned by boiling in a 1:1 mixture of concentrated sulfuric and nitric acid, followed by repeated boiling (four times) with ultrapure water.

The counter electrode consisted of a coiled platinum wire, and the reference consisted of a $Hg/Hg_2SO_4/K_2SO_4$ electrode connected via Luggin capillary. However, all potentials in this article were converted to the RHE scale.

The working electrodes were platinum bead-type single crystals of a Pt[n(111) × (110)] (which is identical to Pt[m(111) × (111)] with $m = n + 1$) orientation, Pt(553) with $n = 4$, Pt(554) with $n = 9$, and Pt(111) with $n = 200-500$, which were prepared according to the method developed by Clavilier et al.[28] Prior to each measurement, the single-crystal electrode was flame annealed and cooled to room temperature in an argon (N50)-hydrogen atmosphere, after which it was transferred to the electrochemical cell under the protection of a droplet of deoxygenated water.[13]

The blank electrolyte consisting of 0.5 M H_2SO_4 was prepared with concentrated sulfuric acid (Merck, "Suprapur") and ultrapure water (Millipore Milli-Q gradient A10 system, 18.2 MΩ cm, 2 ppb total organic carbon). The working solution consisted of the blank electrolyte with 0.025 M methanol (Merck, pro analysi, 99.8%). Argon (N50) was used to deoxygenate all solutions.

All measurements were performed at room temperature (22 °C) using a computer-controlled potentiostat (Eco chemie PGSTAT20, autolab).

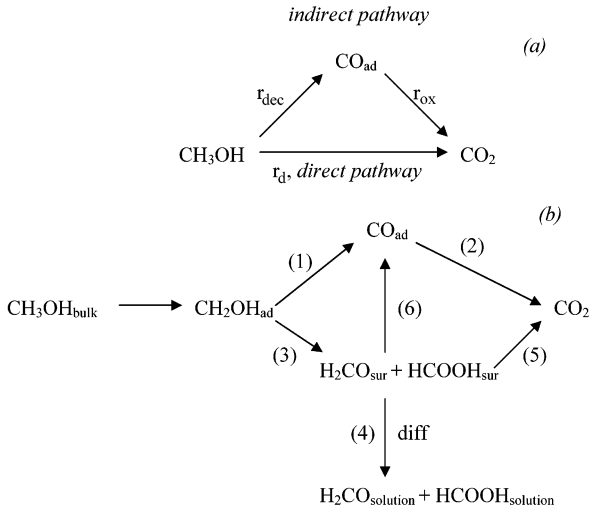

Figure 1. (a) Simplified schematic representation of the parallel pathway for methanol oxidation on platinum electrodes. (b) A more advanced schematic representation of the parallel pathway mechanism for methanol oxidation on platinum electrodes, which incorporates DEMS data on formation on formic acid and formaldehyde.

3. Mechanism and Modeling of the Methanol Oxidation Reaction

Although the decomposition and oxidation reaction of methanol on platinum has been studied extensively in the past, the exact mechanism containing all the reactions and kinetic parameters still remains unclear. Early studies[1] already assumed that the reaction does not proceed through a series of consecutive reactions, but rather proceeds through a parallel path mechanism (see Figure 1a), where the poisoning species, now generally accepted to be surface-bonded carbon monoxide, is formed in an unwanted parallel reaction (indirect pathway, rate r_{dec}). CO_2 may be formed by the direct oxidation of the methanol (direct pathway, rate r_d) or by the oxidation of the adsorbed CO at an increased overpotential (rate r_{ox}). This model has been applied to reactions on single-crystal surfaces by a number of authors.[8,19,23−25,27]

In a chronoamperometric analysis of methanol oxidation on Pt(111), Pt(110), and Pt(100), Franaszczuk and co-workers[25] modeled the poisoning effect, visible in the current−time transients, using only the direct methanol oxidation and CO_{ad} formation reaction from Figure 1a. Their expression for the methanol-related oxidation current recorded in these transients contained four fitting parameters.

$$i(t) = i_{t=0}\left(1 - \frac{\theta_{max}{}^2 k_{dec} t}{1 + \theta_{max} k_{dec} t}\right) + \frac{4 k_{dec} e N_{Pt} \theta_{max}{}^3}{m}\left(\frac{1}{1 + \theta_{max} k_{dec} t}\right)^2 \quad (2)$$

The experiments were designed such that at $t = 0$ the surface could be assumed to be free of poisoning intermediates. In eq 2, $i_{t=0}$ is the initial current density due to the direct oxidation at the unpoisoned surface, k_{dec} is the rate constant of the site blocking process (i.e., decomposition of methanol), θ_{max} is the maximum CO coverage on the surface, e is the elementary charge, N_{Pt} is the surface atom density of Pt(111), and m is the number of surface sites needed to decompose methanol into a CO molecule. On the basis of the least-squares curve fitting results, the most suitable value for m was found to be 2. This equation was able to fit the recorded transients quite well.

A plot of the electrode potential versus the logarithm of the extrapolated initial current yielded a Tafel slope of 120 mV/decade for Pt(110). Combined with the results of an isotope-effect study, the corresponding rate-determining step for methanol oxidation was suggested to be

$$CH_3OH_{(sol)} \xrightarrow{rds} CH_2OH_{(ad)} + H^+ + e^- \qquad (3)$$

Later, Lu et al.[26] modified this model to fit their experiments for methanol oxidation on polycrystalline platinum. After the addition of an exponential current decay to eq 2, which served to account for the rapid decaying current component that is observed in their transients at short times (<40 ms) and was ascribed to species formed during the initial oxidation other than adsorbed CO, they reported a noticeable improvement in the fit.

The apparent success of the Wieckowski group model can be explained by its simplicity and the wide potential range over which it can be used. However, an important element missing in the model is the fact that the oxidation reaction of CO to CO_2 is not incorporated, which may be especially important at higher potentials. Furthermore, as was pointed out by Vielstich et al.,[29] the usage of $i_{t=0}$ as a fitting parameter is somewhat ambiguous. In their analysis of the chronoamperometric transients, Wieckowski et al. found that at potentials where adsorbed CO_{ad} is not oxidized to CO_2, the oxidation current of methanol on Pt(111), Pt(110), and Pt(100) exceeds the current needed to form CO_{ad}. It was assumed that, according to Figure 1a, this excess current was due to the direct formation of CO_2. However, this assumption was disputed by Vielstich et al.,[29] who showed, by using differential electrochemical mass spectrometry (DEMS), that CO_2 evolution occurs only at potentials higher than the CO oxidation potential. This implies that at $t = 0$ methanol does not oxidize completely to CO_2, thus leading to a less straightforward interpretation of the parameter $i_{t=0}$.

To the best of our knowledge, the only model that does incorporate the CO oxidation reaction along with the methanol direct oxidation and decomposition reaction was proposed by Stuve et al.[8,23,24] However, rather than using the chronoamperometric data directly, they chose to model the relationship between the charge obtained from the transients (the reaction charge, q_r), the charge obtained after stripping the electrode of adsorbed species in a different cell (stripping charge, q_s), and time. The results clearly showed that at short times (<30 ms) only partial oxidation products and virtually no CO_2 are formed. At times longer than 5 s, CO_2 production is greatly favored over residue formation. Stuve and co-workers also concluded that for methanol oxidation on Pt(111) electrodes a serial reaction path, involving adsorbed intermediates, is inadequate to describe the observed rate of CO_2 formation. It was proposed that methanol oxidation on CO-covered electrodes proceeds through a parallel pathway mechanism, where the pathway not involving strongly adsorbed species accounts for the majority of the CO_2 produced. This model not only includes the CO oxidation reaction but also is less sensitive to the exact rate equations used to model the system because it uses charge rather than its derivative. Another advantage of this technique is that the stripping charge q_s and, thus, the CO coverage on the electrode surface can be determined accurately. However, unaccounted for is the nature of the intermediate species in the direct methanol oxidation pathway.

In an effort to elucidate the nature of these species and to explain the apparent contradiction between the observations of the groups of Wieckowski and Vielstich, Baltruschat et al.[30,31] proposed a parallel pathway mechanism in which CO_2 could be formed through the oxidation of adsorbed CO or the oxidation of intermediate dissolvable species such as formic acid and formaldehyde. They based their model on DEMS experiments, the results of which clearly showed that H_2CO and HCOOH can be detected during methanol oxidation, and on findings reported by Ota et al.[32] and Iwasita and Vielstich,[33] who already demonstrated the formation of these species under certain conditions. Korzeniewski and Childers showed that during methanol oxidation the formaldehyde yield could be as high as 30%.[34] The resulting more advanced parallel pathway mechanism is schematically depicted in Figure 1b. This mechanism explains the observation of a higher oxidation current than necessary for CO_{ad} formation and the appearance of CO_2 only at potentials higher than the CO oxidation potential, and it incorporates the possibility and identity of intermediate species detected during the incomplete oxidation reaction. Species such as methylformate and 1,1-dimethoxymethane, which were found in small amounts by several groups,[5,31] are not included in this scheme.

In the model we would like to suggest here, the adsorption and subsequent decomposition of methanol and the direct methanol oxidation reaction are treated in the same manner as proposed by Franaszczuk et al.[25] However, instead of assuming that methanol reacts with adsorbed water to form CO_2, six protons, and six electrons (eq 1), we simply assume that a parallel pathway reaction exists, giving rise to a current, i_d. The main difference between our model and that of Franaszczuk et al. is the incorporation of the CO oxidation reaction. The mechanism is, therefore, as follows:

$$CH_3OH \xrightarrow{k_{dec}} CO_{ad} + 4H^+ + 4e^- \qquad \text{decomposition current, } i_{dec} \qquad (4)$$

$$H_2O + {}^* \longleftrightarrow OH_{ad} + H^+ + e^-$$

$$CO_{ad} + OH_{ad} \xrightarrow{k_{ox}} CO_2 + H^+ + e^- + 2^* \qquad \text{oxidation current, } i_{ox} \qquad (5)$$

$$CH_3OH \longrightarrow \text{intermediates} \longrightarrow CO_2 \qquad \text{direct oxidation current, } i_d \qquad (6)$$

$$\text{intermediates} \longrightarrow \text{Diffuse away}$$

The adsorption of water and the subsequent formation of OH_{ad} is assumed to be in equilibrium. The total current is now

$$i = i_d + i_{dec} + i_{ox} \qquad (7)$$

and the rate of surface CO formation and oxidation is given by

$$\frac{d\theta_{CO}}{dt} = k_{dec}(1 - \theta_{CO})^2 - k_{ox}\theta_{CO}(1 - \theta_{CO}) \qquad (8)$$

The second-order decomposition rate law is the same as that used by Franaszczuk et al., whereas the second-order oxidation rate law, which expresses the Langmuir−Hinselwood mechanism underlying CO oxidation, was recently found to satisfactorily fit the CO adlayer oxidation experiments.[35] This differential equation can be solved to yield the following equation for the CO coverage over time:

$$\theta_{CO}(t) = \frac{1 - e^{k_{ox}t}}{1 - (1 + X)e^{k_{ox}t}} \qquad \text{with } X = \frac{k_{ox}}{k_{dec}} \qquad (9)$$

Completing eq 7 gives

$$i(t) = i_d[1 - \theta_{CO}(t)] + 4eN_{Pt}k_{dec}[1 - \theta_{CO}(t)]^2 + 2eN_{Pt}k_{ox}\theta_{CO}(t)[1 - \theta_{CO}(t)] \qquad (10)$$

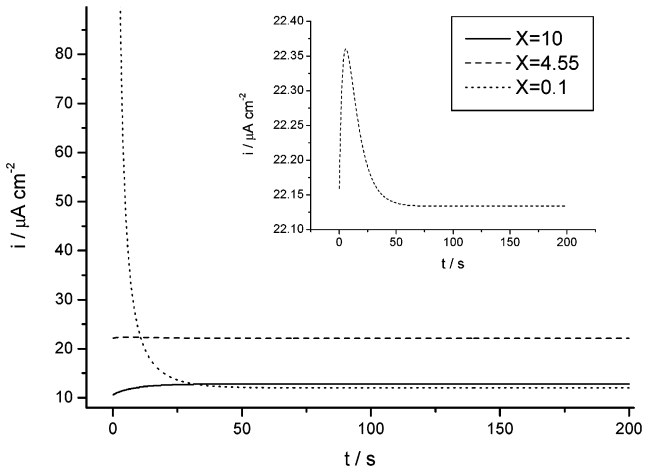

Figure 2. Current−time transient predicted with eq 10 for variable values of X. In all the curves, $i_d = 1 \times 10^{-6}$ A cm^{-2}. For $X = 10$, k_{ox} and k_{dec} are 0.1 and 0.01 s^{-1}, respectively. For $X = 4.55$, these values are 0.1 and 0.022 s^{-1}, and for $X = 0.1$, these values are 0.1 and 1 s^{-1}, respectively.

Here, i_d is the direct oxidation current from reaction 6, k_{dec} is the rate constant for the site blocking process (reaction 4), k_{ox} is the effective oxidation rate constant (reaction 5), N_{Pt} is number of platinum atoms per square centimeter (1.5×10^{15} atoms/cm^2), e is the elementary charge (1.6022×10^{-19} C), and 4 and 2 are the number of electrons involved in the respective reactions. In this model, it is assumed that the maximum coverage of CO on the surface equals 1. Making this assumption allows the differential equation, eq 8, to be solved analytically, and because it only normalizes the CO coverage on the surface, it should not affect the correctness of our model. It should also be noted that in our model, the possible reaction or adsorption of anions and non-CO adsorbates is not taken into account. Equation 10 can be used to fit the chronoamperometric data directly.

An interesting prediction that follows from eq 10 is that the shape of the current transient depends sensitively on the value of X and, thus, on the relative numerical values of k_{ox} and k_{dec}. If i_d is set to 0 at $t = 0$ in eq 10, we can determine a value for X at which the derivative of the function equals 0, namely $X = 4$. Figure 2 demonstrates the effect of the value of X on the shape of the transient. As predicted for $X \geq 4$, the transient changes from a current decreasing with time to a current that increases with time. This means that when the oxidation reaction of CO_{ad} is faster than the methanol decomposition reaction ($X > 4$) we would expect the recorded current to increase due to a slow increase in CO coverage, which is then rapidly oxidized. It is interesting to see that for values a little higher than 4 the curve can go through a maximum, as is shown in the inset in Figure 2. In this situation, the initial CO oxidation reaction is fast but slows down after some time as a result of an increased poisoning of the surface. For $X < 4$, we obtain the expected decreasing current transient, as also predicted by eq 1. Experimentally, we expect the condition of $X > 4$ to be most easily satisfied by working at a low methanol concentration.

Because of the incorporation of the CO oxidation reaction, the potential range for which our model can be applied should be considerably broader than that for Franaszczuk et al.'s model. Of course, setting the current produced in the direct pathway equal to i_d, without making any assumptions regarding the nature of the reaction steps, the amount of electrons produced per methanol molecule, or the formed products, is a not an improvement over the previous model. Nevertheless, because

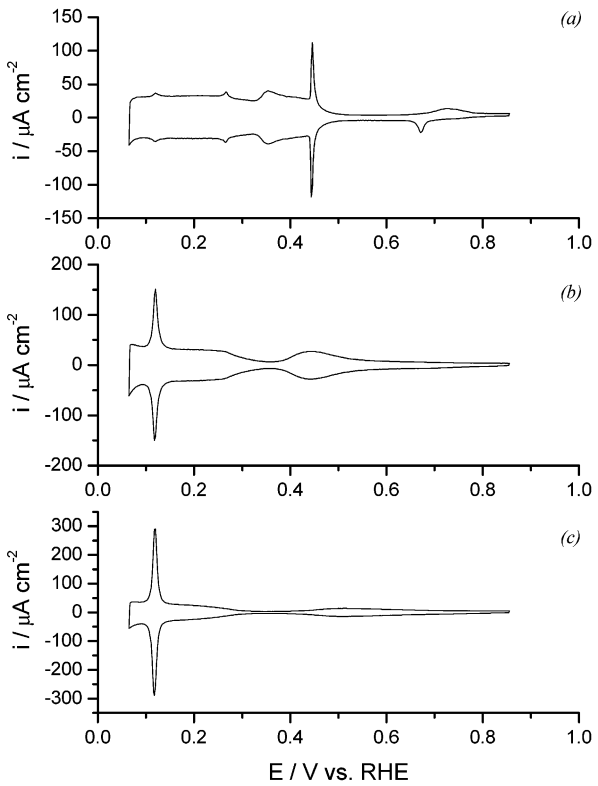

Figure 3. Cyclic voltammograms of Pt(111) (a), Pt(554) (b), and Pt(553) (c) in 0.5 M H_2SO_4. The sweep rate was 50 mV/s.

Wang et al.[30,31] showed that the contribution of the direct pathway can be considerable on CO-covered electrode surfaces, the addition of i_d is more or less a necessity.

4. Results and Discussion

4.1. Cyclic Voltammetry. As is customary for single-crystal experiments, the cleanliness of the system was checked by recording a cyclic voltammogram of the electrode in contact with the blank electrolyte. The cyclic voltammogram of Pt(111) in 0.5 M H_2SO_4 is shown in Figure 3a. It shows the characteristic well-developed sharp "butterfly" peak at 0.45 V, which is ascribed to the sulfate adlayer disorder−order phase transition[36,37] and has only small amounts of (110) and (100) defects, as can be seen from the two small peaks in the hydrogen adsorption/desorption region at 0.125 and 0.27 V.[38]

Both stepped surfaces in Figure 3b,c show sharp peaks at 0.125 V due to the adsorption and desorption of hydrogen on the (110) steps[39] (although Marković et al. have claimed that the pseudocapacitance under this peak corresponds not only to hydrogen adsorption/desorption but also to adsorption/desorption of (bi)sulfate),[40,41] while the broad features negative of 0.35 V and positive of 0.4 V are due to hydrogen and sulfate adsorption/desorption on the terraces, respectively.[11,42,43] All the recorded blank cyclic voltammograms are in good correspondence with those previously reported in the literature and satisfy the criteria of system cleanliness proposed by Lebedeva et al.[11]

Cyclic voltammograms of the three electrodes in methanol containing electrolyte compared to the blank voltammograms are shown in Figure 4. When examining the hydrogen region on the stepped crystals, it can be noticed that the hydrogen adsorption/desorption on the steps is affected most by the presence of methanol and that for Pt(111) the signals corresponding to the (110) and (100) defect sites have disappeared (see Figure 4a). This can be rationalized by assuming that either

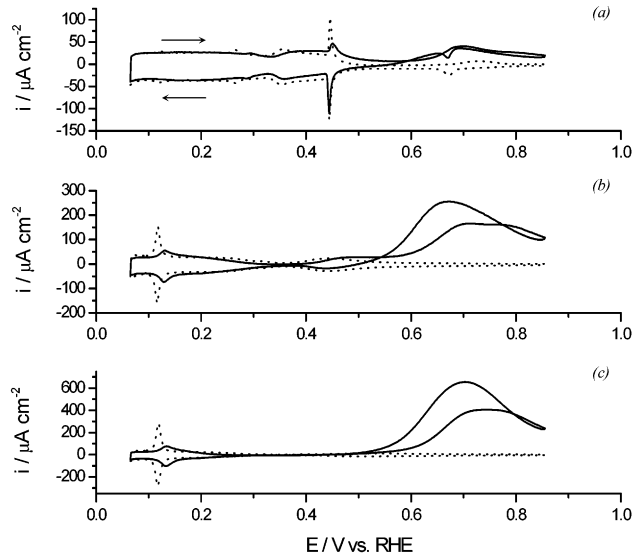

Figure 4. Cyclic voltammograms for the Pt(111) (a), Pt(554) (b), and Pt(553) (c) in 0.5 M H_2SO_4 (dotted line) and in 0.5 M H_2SO_4 + 0.025 M CH_3OH (continuous line). The sweep rate was 50 mV/s.

methanol or a species formed in the decomposition reaction adsorb preferentially at the defect sites. It can also be seen that at this sweep rate the sulfate disorder−order transition peak is largely suppressed in the positive-going sweep on Pt(111), indicating that species, again probably adsorbed CO, are present on the terraces. However, from these observations little can be said about where methanol preferably decomposes. In the returning sweep, the disorder−order peak is no longer suppressed, indicating that sulfate is the most abundant species on the terraces and previously adsorbed species have been removed. The (110) and (100) defects in the hydrogen region remain absent in the negative-going sweep, again indicating that methanol either preferably adsorbs or decomposes on the steps or that the decomposition products diffuse over the surface and get trapped in the defect sites.

On the stepped surfaces, the negative-going sweep shows virtually no difference with the positive-going sweep (see Figure 4b,c). Apparently, at this sweep rate the adsorption/decomposition reaction on stepped electrodes is fast enough to "refill" the steps again after the oxidation of adsorbed species occurred at higher potentials. However, it is noteworthy that in the voltammograms recorded in MeOH containing electrolyte on the stepped surfaces the hydrogen peak corresponding to the steps is shifted to more positive potentials when compared to the blank cyclic voltammogram. This suggests that the adsorption of hydrogen is easier in the presence of adsorbed methanol or CO on the steps. A similar effect is also observed when only CO is adsorbed on these surfaces.[11] Also noteworthy is the fact that for Pt(111) the two small peaks at approximately 0.7 V in the positive- and negative-going sweep, which have been ascribed to OH formation and subsequent reduction,[44,45] are still visible in the voltammogram. This indicates that, at this methanol concentration, OH species, which are not used in oxidizing adsorbed CO, are formed on the surface.

Judging from the methanol oxidation current densities recorded on these electrodes, the order in the reaction rate is Pt(111) < Pt(554) < Pt(553), thus hinting at the fact that the oxidation reaction is structure-sensitive and that the rate of the reaction increases with the step density. We also find that the current at the onset of methanol oxidation increases for an increasing step density. This is contrary to the findings of Tripković and Popović, who reported that the initial surface activity for methanol on Pt(755), Pt(211), and Pt(311) decreases for an increasing step density.[21] However, this difference may be due to the fact that these authors used an electrode type different (Pt[n(111) × (100)]-type electrodes) from ours (Pt-[n(111) × (110)]-type electrodes). In a study of methanol oxidation on low-index platinum single crystals performed by Herrero et al.,[19] methanol was found to react slower on Pt(100) than on Pt(110). For Pt(110) and Pt(100), different values for the Tafel slope were found (120 and 60 mV/decade, respectively) indicating a difference in the rate-determining step, which may account for the difference in observations. Our observation compared to the results of Tripković and Popović may indicate that methanol decomposes significantly faster at the (110) than at the (100) steps. Interestingly, in an infrared study on CO oxidation on stepped single crystals, Lebedeva et al.[46] found no significant difference in the reactivity of CO oxidation on electrodes with either the (110) or the (100) steps.

The important question is now which reaction is observed at a certain potential: the methanol decomposition reaction, the direct methanol oxidation reaction (pathways 3−5, Figure 1b), or the indirect pathway via CO oxidation (pathways 1 and 2, Figure 1b)? Of these three reactions, the decomposition reaction as well as the CO oxidation reaction are known to be structure-sensitive,[11] and the direct methanol oxidation reaction may be as well. We attempt to address this issue with the help of chronoamperometry in the next section.

4.2. Chronoamperometry. After the addition of 0.025 M MeOH and prior to the chronoamperometric measurement, the single crystal was cleaned of preadsorbed methanol decomposition products by stepping the potential from a potential in the hydrogen region (0.085 V) to 0.855 V for 20 s. It is assumed that at this potential all the preadsorbed products are oxidized and the electrode is effectively cleaned of preadsorbed species. Directly after the cleaning procedure, the potential was stepped down to the desired potential and the current−time transient was recorded.

Transients were recorded from 0.305 to 0.805 V with a potential step increase of 50 mV per experiment. In the range of 0.655−0.755 V, four additional data series at 0.675, 0.690, 0.720, and 0.735 V were recorded. All the measurements were performed at least three times.

Some examples of the resulting chronoamperometric curves can be found in Figure 5. The current−time curves shown were recorded at 0.655, 0.705, 0.755, and 0.805 V versus the RHE in 0.5 M H_2SO_4 and 0.025 M methanol. Comparing the current densities measured in the transients with the current densities given by the Cottrell equation shows that the reaction is not diffusion limited.[47]

The transients for the methanol decomposition on Pt(554) and Pt(553) show a current decrease in the first 200 s, followed by a more or less constant current at longer times. These transients resemble the transients recorded by Wieckowski et al. and Stuve et al.[8,23−27] on Pt(111) in 0.5 M H_2SO_4 and 0.2 M methanol. However, for potentials below about 0.7 V, the curve for Pt(111) shows an increase in current in the first 50−100 s before reaching the steady-state current. Above this potential, the initial shape of the transient becomes flatter, though a change to an initial current decrease analogous to the stepped crystals cannot be observed unambiguously. This anomalous shape may be rationalized by assuming that the oxidation rate of chemisorbed intermediates is higher than the decomposition rate of methanol because of the low methanol concentration in our experiments. In this case, the value for X in our model should

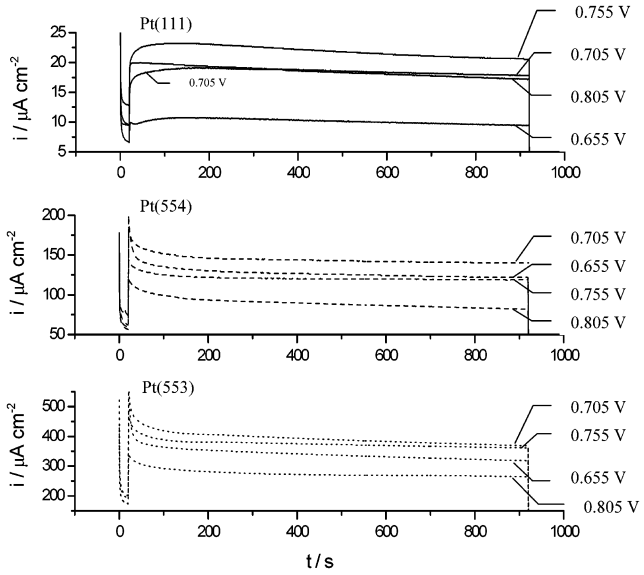

Figure 5. Current transients of the decomposition of methanol on Pt(111) (continuous line), Pt(554) (dashed line), and Pt(553) (dotted line). The step potentials are 0.655, 0.705, 0.755, and 0.805 V versus the RHE.

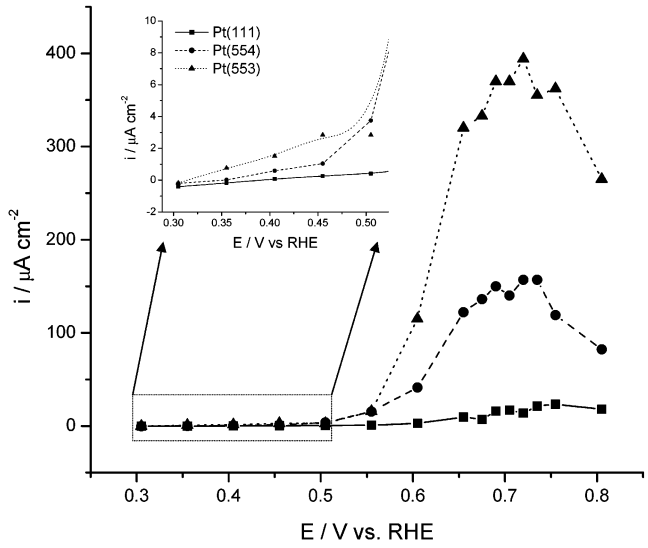

Figure 6. Steady-state current, i_{ss}, of the methanol decomposition/oxidation on Pt(111) (■), Pt(554) (●), and Pt(553) (▲) in 0.5 M H_2SO_4 and 0.025 M methanol. The steady-state current was recorded from the chronoamperometric transients at $t = 900$ s. Enlarged is the steady-state current−potential relationship at low potentials.

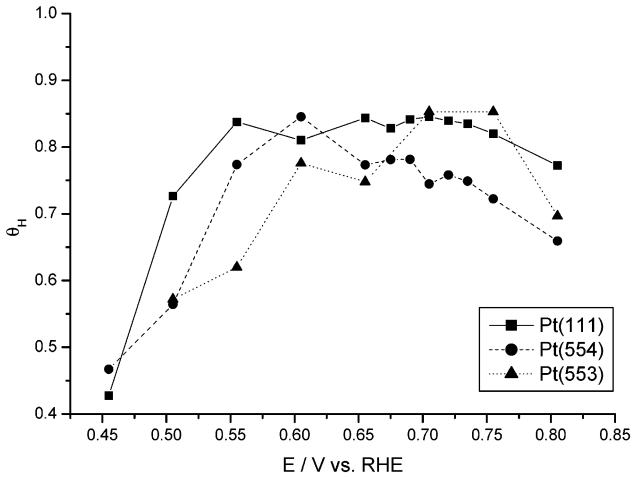

Figure 7. Hydrogen coverage versus the step potential on Pt(111) (■), Pt(554) (●), and Pt(553) (▲). The coverage was determined from the hydrogen adsorption/desorption charge obtained from a cyclic voltammogram of the hydrogen region. The cyclic voltammogram was recorded at 750 mV/s in the methanol-containing electrolyte. Each point is the average of three experiments.

be well over 4. Note that at the applied potentials oxygen-containing surface species should react much faster than a few seconds and, therefore, the associated reduction current cannot explain the shape of the recorded transients. Note also that the qualitative shape of the transients on Pt(111) can be explained by our model but not by the models suggested by Franaszczuk et al.[25] and Lu et al.[26]

The data shown in Figure 5 clearly demonstrate that increasing the step density leads to an increase in the overall current. This is true for the entire potential range under investigation at all times during the transient. Also, in general, the steepness of the initial current drop increases for an increasing step density, which means that surfaces with a high amount of (110) steps poison faster than surfaces with little or no defects, again indicating that the reaction is highly structure-sensitive, in agreement with the literature.[14,15,18,20]

A plot of the current measured at $t = 900$ s versus the step potential is shown in Figure 6. The enlarged area shows the behavior at low potentials. It is immediately clear that all three surfaces exhibit nearly the same qualitative trends over the entire potential region. First, the steady-state current increases slightly with the potential when going from 0.3 to 0.5 V, followed by a drastic increase at higher potentials up to approximately 0.7 V. At potentials above about 0.7−0.75 V, the current decreases again for all three electrodes.

Taking into consideration our model for methanol decomposition and subsequent oxidation, this trend can be rationalized by assuming that at low potentials the CO oxidation is the rate-determining step and increases only weakly with increasing potentials below 0.5 V. When the potential is higher than 0.5 V, the CO oxidation reaction proceeds faster and the current increases rapidly. It can be assumed that the rate-determining step is now the adsorption/decomposition of methanol on the surface. The subsequent decrease in the steady-state current for potentials higher than 0.7−0.75 V is generally ascribed to a decrease in free adsorption sites for methanol as a result of an increasing OH coverage.[1]

4.3. Surface Species Coverage. Directly after the steady-state measurements, a cyclic voltammogram of the hydrogen region was recorded to have an indication of the hydrogen coverage and, thus, indirectly of the coverage of adsorbed species on the surface. The relationship between hydrogen and coadsorbed CO on the investigated single crystals has been determined empirically by Lebedeva et al.[35] The cyclic voltammograms were recorded in the methanol-containing electrolyte at a scan rate of 750 mV/s to ensure that the renewed adsorption of methanolic species on the surface during the scan is negligible. The resulting relationship between the hydrogen coverage and the step potential is shown in Figure 7. Admittedly, this procedure is not the most accurate for determining the coverage of adsorbed species (presumably mostly CO), but it avoids cumbersome transfer experiments and the qualitative general trends can still be useful.

Clearly, at low potentials the number of free sites for hydrogen to adsorb is limited, meaning that the coverage of decomposition products is high. Assuming that CO is the primary decomposition product, this is in agreement with our previous explanation that at these potentials the CO oxidation

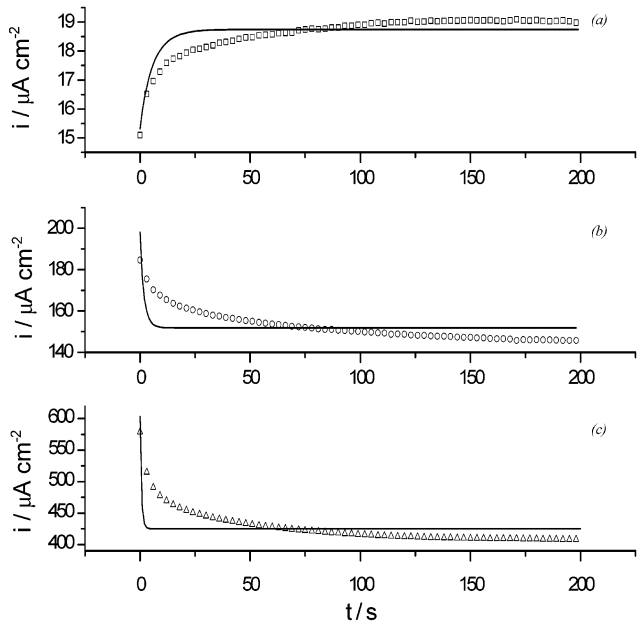

Figure 8. Current transients for methanol decomposition fitted with our model *without* i_d (continuous line) on Pt(111) (a), Pt(554) (b), and Pt(553) (c). The transients shown were recorded at 0.705 V versus the RHE in 0.5 M H_2SO_4 and 0.025 M CH_3OH.

reaction is slow and rate-determining. Also, it can be observed that below 0.6 V the amount of adsorbed species on the electrode surface generally increases with an increasing step density.

At potentials above 0.6 V, the coverage of adsorbed decomposition species becomes much lower, which implies that the formed carbon monoxide reacts off the surface rapidly and methanol decomposition has become rate-limiting. This is consistent with our previous interpretation of the data in Figure 6.

4.4. Modeling the Chronoamperometric Data. Both eq 2 and our model eq 10 were used to fit the chronoamperometric data of the methanol decomposition and oxidation on the single-crystal electrodes. Of our model, two versions were used: version 1 excludes the direct current, i_d, and version 2 includes i_d. Only the first 200 s of the transients were used in the fitting procedure, because for $t > 200$ s the current still decreases slowly but continuously. Whether this decrease results from the methanol-related reactions occurring at the electrode surface or from the blockage of reactive sites due to adsorption of contaminating species is still unclear. Examples of the fit produced by version 1 are shown in Figure 8, while the fits produced by version 2 and Franazczuk et al.'s model can be found in Figure 9. The graphs of the obtained values for the variable parameters versus the step potential found with the various models are shown in Figures 10 and 11. Values for k_{dec} and k_{ox} resulting from version 1 of our model are given in Figure 10a, while the values for i_d and k_{dec} and k_{ox} obtained from version 2 are presented in parts b and c of Figure 10, respectively. Parts a−c of Figure 11 present plots of θ_{max}, log($i_{t=0}$), and k_{dec}, respectively, versus the potential, obtained from the model of Franaszczuk et al., eq 2.

Examination of the curve fitting shown in Figures 8 and 9 reveals that, unlike both versions of our model, the model proposed by Franaszczuk et al. is not able to predict the initial current increase measured on the Pt(111) electrode because of the absence of the CO oxidation reaction in this model. Interestingly, the introduction of another reaction parameter in our model, namely, i_d, has almost no influence on the curve

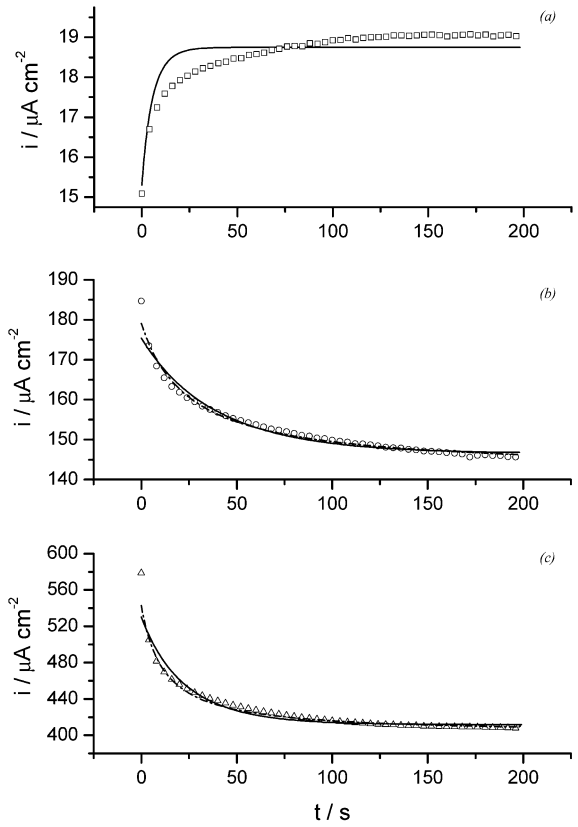

Figure 9. Current transients for methanol decomposition fitted with our model *with* i_d (continuous line) and Franaszczuk et al.'s model (dotted line) on Pt(111) (a), Pt(554) (b), and Pt(553) (c). The transients shown were recorded at 0.705 V versus the RHE in 0.5 M H_2SO_4 and 0.025 M CH_3OH.

fitting for the (111) surface. The reason for the lack of an important influence of i_d on the fit is that the CO coverage under these conditions is very low, meaning that the term $i_d(1 - \theta)$ in eq 10 is essentially constant. Because the poorness of the fit is related to the time-dependence of the current rather than the absolute values, adding i_d makes no great difference. It seems that the direct pathway current is very small on the essentially defect-free Pt(111) for a low methanol concentration, as can be deduced from Figure 10b, which shows that for Pt(111) the value for i_d is very low over the entire potential region under investigation. We note that the fits shown in Figure 8 cannot be improved by changing the total time over which the current is fitted. The reason for the poor fits obtained with version 1 of our model is more fundamental. Whereas the transients produced with version 1 of our model are approximately exponential [$i(t) = A + Be^{(-kt)}$], a log−log analysis of the experimental transients show that they follow more closely a power-law-type description [$i(t) = A + Bt^{\alpha}$].

On stepped surfaces, however, incorporating the direct current in the model greatly improves the accuracy of the fit. When comparing Franaszczuk et al.'s model with version 2 of our model, one is inclined to say that the former produces a somewhat better fit. However, as we will argue in the following, we believe this better fit is mainly the result of the fact that their fit parameter θ_{max} gives more flexibility to the fit than our k_{ox}. We also tested if the fit of our model (version 2) would be more accurate if the time interval under investigation is shortened to the first 50 s of the transients instead of the first 200 s. Performing the same transient analysis again on the stepped electrodes for $t \leq 50$ s showed that also for this

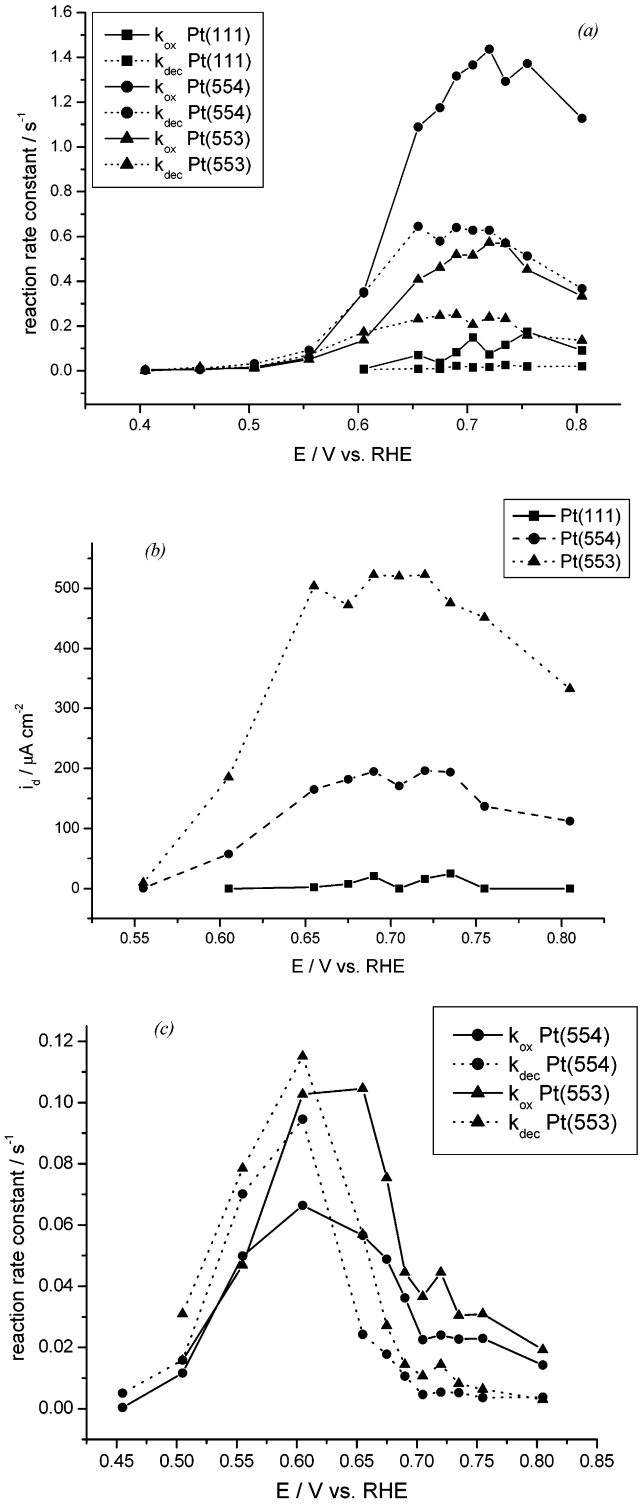

Figure 10. (a) CO oxidation rate constant, k_{ox} (continuous line), and methanol decomposition rate constant, k_{dec} (dotted line), versus the potential on Pt(111) (■), Pt(554) (●), and Pt(553) (▲) obtained from our model without i_d. (b) Direct methanol oxidation current, i_d, determined by our model on Pt(111) (■), Pt(554) (●), and Pt(553) (▲) in 0.5 M H_2SO_4 and 0.025 M methanol. (c) CO oxidation rate constant, k_{ox} (straight line), and methanol decomposition rate constant, k_{dec} (dotted line), versus the potential on Pt(554) (●) and Pt(553) (▲) obtained from our model with i_d.

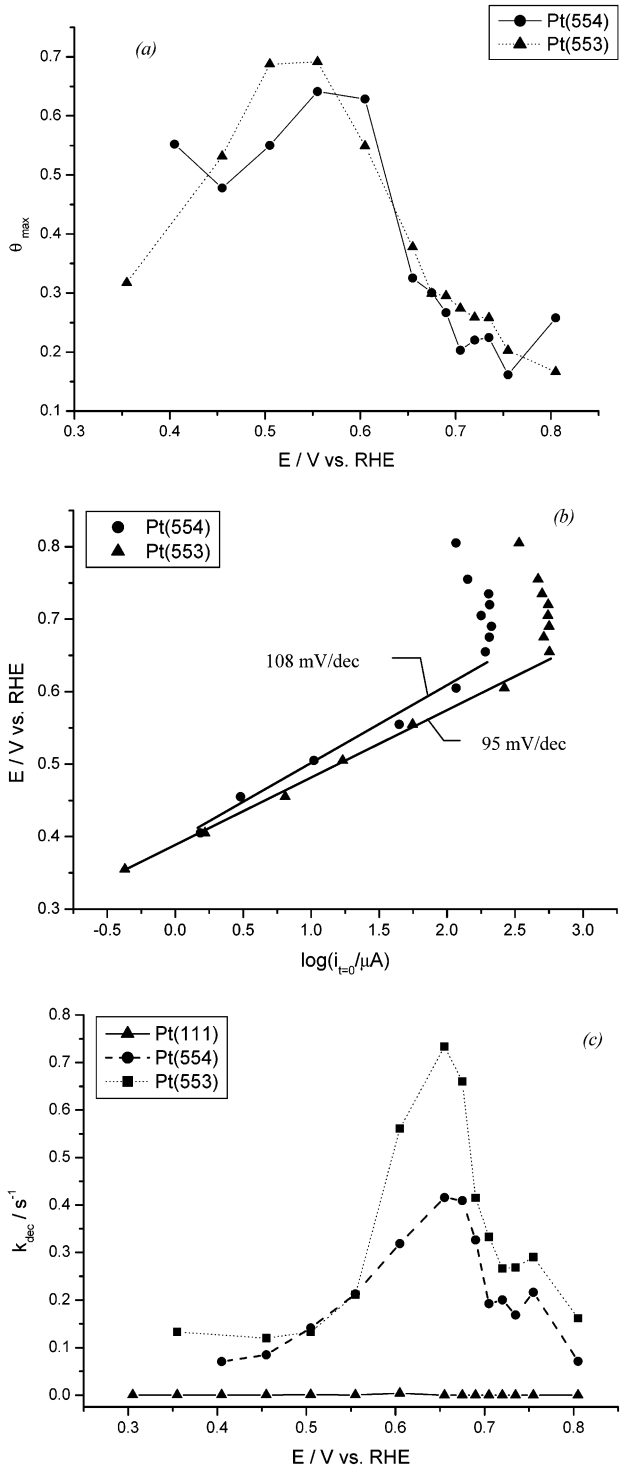

Figure 11. (a) Maximum CO coverage on Pt(554) (●) and Pt(553) (▲) obtained by fitting with eq 2. (b) Electrode potential versus log-($i_{t=0}$) for methanol decomposition/oxidation on Pt(554) (●) and Pt-(553) (▲) in 0.5 M H_2SO_4 and 0.025 M CH_3OH. (c) Dependence of the adsorption rate constant, k_{dec}, obtained by fitting with eq 2, on the potential.

shortened time interval Franaszczuk et al.'s model gives a more accurate fit of the data.

In their model, Franaszczuk et al. used the maximum CO coverage on the surface as a variable, whereas theoretically this value would be expected to be virtually potential-independent.[25] Only after the addition of an exponential decay factor to eq 2 did the same group[26] report a potential-independent θ_{max}. When fitting our chronoamperometric data with eq 2, the resulting θ_{max} is not potential-independent, as can be seen from Figure 11a. For the stepped surfaces, the calculated maximum CO coverage increases to about 0.7 when increasing the potential from 0.4 to 0.55 V, after which it drops again to an unrealisti-

cally low value of approximately 0.2 when the potential is further increased from 0.55 to 0.8 V. (Due to the current increase observed on Pt(111), eq 2 produced unrealistic values for the fitted parameters. These values were, therefore, omitted from Figure 11a,b.) This demonstrates that θ_{max} is an important parameter necessary for an accurate fit of the data, which, we believe, should not be the case.

Following Franaszczuk et al., a Tafel slope for the direct current can be obtained by plotting $\log(i_{t=0})$ versus E (Figure 11b). After applying their model to our data, we find Tafel slopes for Pt(554) and Pt(553) of 110 and 95 mV/decade, respectively, in the potential range from 0.405 to 0.655 V. These values are close to those reported by Franaszczuk et al., who found Tafel slopes of 106 and 120 mV/decade for Pt(111) and Pt(110), respectively, in 0.1 M H_2SO_4 and 0.2 M methanol. The slight deviation may be caused by the fact that we chose not to correct our transients with a current transient recorded in the blank electrolyte.

The fit results shown in Figure 10 confirm the qualitative conclusions drawn in the previous sections. The results obtained for the decomposition and oxidation rate constants from both version 1 and version 2 indicate that the steps and defects catalyze methanol decomposition and subsequent CO oxidation, suggesting that both processes take place preferentially at the steps. Note that the rate constants obtained with version 1 are substantially higher than those obtained with version 2 of the model as a result of the absence of the direct path in the former. Another observation to be made from Figure 10a,b is the existence of the transition potential of about 0.6−0.65 V. Below this potential, decomposition is fast compared to oxidation, whereas above this potential, oxidation is faster than decomposition. The existence of this transition potential is related to the low methanol concentration used in our experiments. This is again in good accordance with our previous deductions. At this point, we would like to remark that the values found for the CO oxidation rate constant lie within the range of $10^{-2}-10^{2}$ s^{-1}, which agrees well with the CO oxidation rate constants on these surfaces determined experimentally by Lebedeva et al.[35]

The results shown in Figure 10b would suggest that the direct pathway is also strongly structure-sensitive and dictated by a process that takes place preferentially at the step sites. The plot of i_d versus the step potential shown in Figure 10b closely resembles that of the steady-state current in Figure 6, the only difference being that the direct methanol current is higher than the measured steady-state current. On all the surfaces, the direct current is virtually zero for potentials below 0.55 V, while it rises fast for potentials over 0.6 V to fall again after a potential of 0.7 V has been reached. This finding is in agreement with recent data reported by Wang et al.,[30,31,48] who revealed that the formation of formic acid and formaldehyde starts at a potential of about 0.6 V and reaches a maximum at a potential, which coincides with the maximum of the methanol oxidation peak recorded in the cyclic voltammogram.

The reason for i_d being higher than the steady-state current may be found in the fact that the steady-state current was recorded at approximately $t = 900$ s while the direct current was determined by modeling the transient in the first 200 s. In the remaining 700 s the current still changes, which can account for the discrepancy.

Figure 11 shows the results obtained for the potential dependence of the fit parameters in Franaszczuk et al.'s model eq 2. The results in Figure 11b,c confirm that both the decomposition rate and the direct current increase with an increasing step density. We do believe, however, that for potentials higher than about 0.6−0.65 V, the model is less applicable to the actual process because above these potentials CO oxidation (the indirect pathway) can no longer be neglected. We believe that this is the reason for the sudden drop found in k_{dec} (Figure 11c) and especially θ_{max} (Figure 11a) above 0.6−0.65 V. The almost instantaneous drop in θ_{max} from 0.6 to 0.7 (which seems a reasonable number) to about 0.2 is unrealistic and in our view must be due to a process that takes place at potentials above 0.6−0.65 V, which is not incorporated in the model. Note that this transition potential of 0.6−0.65 V is exactly the potential for which the fits to our model suggest that CO oxidation (and, hence, the indirect pathway) becomes a fast process. Also, the strong potential dependence of θ_{max} suggests that it is a powerful fit parameter, which may explain why the fits obtained with eq 2 are always slightly better than those produced with eq 10. However, because such a potential dependence does not seem realistic, it can be questioned whether this more accurate fit is also physically more meaningful.

Finally, we would like to conclude this section with a strong word of caution regarding the fitting of chronoamperometric methanol oxidation transients. We have used the mathematical model presented in section 3 mainly for two purposes. First, the model explains the rising transients obtained on Pt(111) at low methanol concentrations as a consequence of the combination of slow decomposition and rapid subsequent oxidation of the decomposition product. Second, the fitting helped in substantiating the qualitative conclusions of the earlier sections, namely, that both the methanol decomposition and poison oxidation take place preferentially at the steps and that for the methanol concentration used here there is transition potential of about 0.6−0.65 V at which there is a change in the rate-determining step from decomposition to oxidation. The fit results also suggest that the direct pathway is catalyzed by step sites, which may in fact be interpreted as methanol decomposition and methanol direct oxidation going through the same initial intermediates, as is suggested by the scheme in Figure 1b. However, the accuracy of the rate parameters obtained with the model, and especially those for the direct pathway, remains highly questionable. For instance, it is known from the literature that the amount of formic acid and formaldehyde detected depends on the flow rate and the methanol concentration of the electrolyte solution. Because in our system convection is absent and the methanol concentration is rather low, which, according to the data reported in the literature, would favor the direct pathway, it may be argued whether the introduction of i_d, or the model employed for it, is justified. This problem can only be solved by measuring the direct pathway by another method simultaneously, for instance using on-line mass spectrometry. Furthermore, the actual rate laws employed in eq 8 for methanol decomposition and subsequent CO oxidation may be incorrect or oversimplified. The "ensemble effect" suggested by the quadratic dependence of the decomposition rate on the number of free sites is still poorly understood. The Langmuir−Hinselwood kinetics assumed for CO oxidation is known to give satisfactory results for high CO coverages but is much less accurate for the oxidation of submonolayer coverages of CO, as was discussed by Lebedeva et al.[35] Unfortunately, the low CO coverage regime seems to be the relevant one for the experiments presented here. As long as these uncertainties regarding the importance of the direct pathway and the most accurate rate laws for describing the different processes exist, modeling and fitting methanol oxidation transients should only be used as an additional tool to put qualitative conclusions obtained by other methods on a semiquantitative footing.

5. Conclusion

The methanol oxidation reaction has been studied on Pt-[n(111) × (110)]-type electrodes in a 0.5 M H_2SO_4 solution with 0.025 M CH_3OH. By combining voltammetry, chronoamperometry, and the fitting of the chronoamperometric transients with a new mathematical model incorporating methanol decomposition, poison oxidation, and methanol direct oxidation, we have shown that the methanol oxidation reactivity is strongly catalyzed by the presence of step and defect sites. The cyclic voltammetry data showed that the overall oxidation rate increases with an increasing step density. Moreover, the defect or step sites on all surfaces are affected by the presence of methanol more than the terraces sites. This implies that either the decomposition products of methanol or the methanol itself preferably sits at the steps.

Analysis of the chronoamperometric data shows that the steady-state activity increases with an increasing step density over the entire potential range. The drop in transient activity is faster on a surface with a higher step density, suggesting that the methanol decomposition into the CO poisoning species takes place preferentially at or near steps. From the observation that the CO coverage at the end of the transient is low for potentials higher than 0.55 V, it is concluded that the CO oxidation is faster at these potentials, whereas at lower potentials methanol decomposition is faster than CO oxidation. The mathematical model predicts that when CO oxidation is faster than methanol decomposition, a rising current transient should be obtained, which has indeed been observed for Pt(111). The decomposition rate on this surface is low because of the low defect density and because of the low methanol concentration used in our experiments. Fitting the transients to our mathematical model suggests that methanol decomposition, CO oxidation, and methanol direct oxidation are catalyzed by the steps. The fit results also confirm the transition from CO oxidation being rate-determining below about 0.6 V to methanol decomposition being rate-determining above this potential.

The mathematical model suggested in the paper presents an extension and, we believe, an improvement over an earlier model for fitting chronoamperometric data, suggested by Franaszczuk et al.,[25] because their model does not incorporate the CO oxidation process. However, fitting methanol oxidation transients remains a problematic and potentially deceptive undertaking. First of all, the correct rate laws for both methanol decomposition and CO oxidation at low CO coverage are not well-known. It may be mentioned that the coulometry-based method proposed by Stuve et al. partially circumvents this problem because the time-dependent charge is presumably less sensitive to the exact nature of the rate laws than the time-dependent current. Second, the direct methanol pathway and especially its intermediates and final products as a function of the potential and other variables of the system need to be much better documented and understood to perform meaningful quantitative modeling. In this respect, it would clearly be a substantial improvement if the present experiments could be augmented by transient on-line mass spectroscopy.

Nevertheless, despite these reservations, we believe our results strongly suggest that steps of a (110) orientation catalyze the methanol decomposition, the CO oxidation, and presumably also the direct methanol oxidation. The latter process may in fact be related to the initial stages of the methanol decomposition. Our observations seem to be in conflict with the earlier results of Tripković et al.,[21] who found that an increasing density of steps of a (100) orientation leads to a lower methanol oxidation activity. This difference may be due to a different methanol concentration or due to the different orientation of the steps because the Pt(100) surface is indeed known to be much less active for methanol oxidation than the Pt(110) surface. Hence, the elucidation of the role of methanol concentration and the effect of the step orientation is an important goal for future work. Finally, because it is known that the methanol oxidation currents on the three basal planes of platinum are very sensitive to the electrolyte anion, a systematic study comparing the activity of stepped Pt in sulfuric and perchloric acid with different concentrations of methanol would be very valuable.

Acknowledgment. This research was supported by The Netherlands Foundation for Scientific Research (NWO). Special thanks go to Professor Juan Feliu of the Departamento de Química-Física at University of Alicante in Spain for supplying the stepped single crystals.

References and Notes

(1) Parsons, R.; VanderNoot, T. *J. Electroanal. Chem.* **1988**, *257*, 9.
(2) Kizhakevariam, N.; Stuve, E. M. *Surf. Sci.* **1993**, *286*, 246.
(3) Hopranyi, G.; Wieckowski, A. *Proc. Electrochem. Soc.* **1992**, *92*, 70.
(4) Marković, N. M.; Ross, P. N. *Surf. Sci. Rep.* **2002**, *45*, 117.
(5) Iwasita, T. *Electrochim. Acta* **2002**, *47*, 3663.
(6) Hamnett, A. *Comp. Chem. Kin.* **1999**, 635.
(7) Wasmus, S.; Küver, A. *J. Electroanal. Chem.* **1999**, *461*, 14.
(8) Jarvi, T. D.; Sriramulu, S.; Stuve, E. M. *J. Phys. Chem. B* **1997**, *101*, 3649.
(9) Marković, N. M.; Lucas, C. A.; Rodes, A.; Stamenkovic, V.; Ross, P. N. *Surf. Sci.* **2002**, *499*, L149.
(10) Beden, B.; Lamy, C.; De Tacconi, N. R.; Arvia, A. J. *Electrochim. Acta* **1990**, *35*, 691.
(11) Lebedeva, N. P.; Koper, M. T. M.; Herrero, E.; Feliu, J. M.; van Santen, R. A. *J. Electroanal. Chem.* **2000**, *487*, 37.
(12) Lebedeva, N. P.; Koper, M. T. M.; Feliu, J. M.; van Santen, R. A. *J. Phys. Chem. B* **2002**, *106*, 12938.
(13) Lebedeva, N. P.; Koper, M. T. M.; Feliu, J. M.; van Santen, R. A. *Electrochem. Commun.* **2000**, *2*, 487.
(14) Gibson, K. D.; Dubois, L. H. *Surf. Sci.* **1990**, *233*, 59.
(15) Desai, S. K.; Neurock, M.; Kourtakis, K. *J. Phys. Chem. B* **2002**, *106*, 2559.
(16) Clavilier, J.; Durand, R.; Guinet, G.; Faure, R. *J. Electroanal. Chem.* **1981**, *127*, 281.
(17) Lamy, C.; Léger, J. M.; Clavilier, J.; Parsons, R. *J. Electroanal. Chem.* **1983**, *150*, 71.
(18) Xia, X. H.; Iwasita, T.; Ge, F.; Vielstich, W. *Electrochim. Acta* **1996**, *41*, 711.
(19) Herrero, E.; Franaszczuk, K.; Wieckowski, A. *J. Phys. Chem. B* **1994**, *98*, 5074.
(20) Shin, J.; Korzeniewski, C. *J. Phys. Chem. B* **1995**, *99*, 3419.
(21) Tripković, A. V.; Popović, K. D. *Electrochim. Acta* **1996**, *41*, 2385.
(22) Park, S.; Xie, Y.; Weaver, M. J. *Langmuir* **2002**, *18*, 5792.
(23) Sriramulu, S.; Jarvi, D.; Stuve, E. M. *Electrochim. Acta* **1998**, *44*, 1127.
(24) Sriramulu, S.; Jarvi, T. D.; Stuve, E. M. *J. Electroanal. Chem.* **1999**, *467*, 132.
(25) Franaszczuk, K.; Herrero, E.; Zelenay, P.; Wieckowski, A.; Wang, J.; Masel, R. I. *J. Phys. Chem. B* **1992**, *96*, 8509.
(26) Lu, G. Q.; Chrzanowski, W.; Wieckowski, A. *J. Phys. Chem. B* **2000**, *104*, 5566.
(27) Herrero, E.; Chrzanowski, W.; Wieckowski, A. *J. Phys. Chem.* **1995**, *99*, 10423.
(28) Clavilier, J.; Armand, D.; Sun, S. G.; Petit, M. *J. Electroanal. Chem.* **1986**, *205*, 267.
(29) Vielstich, W.; Xia, X. H. *J. Phys. Chem.* **1995**, *99*, 10421.
(30) Wang, H.; Wingender, C.; Baltruschat, H.; Lopez, M.; Reetz, M. T. *J. Electroanal. Chem.* **2001**, *509*, 163.
(31) Wang, H.; Löffler, T.; Baltruschat, H. *J. Appl. Electrochem.* **2001**, *31*, 759.
(32) Ota, K.-I.; Nakagawa, Y.; Takahashi, M. *J. Electroanal. Chem.* **1984**, *179*, 179.
(33) Iwasita, T.; Vielstich, W. *J. Electroanal. Chem.* **1986**, *201*, 403.
(34) Korzeniewski, C.; Childers, C. L. *J. Phys. Chem. B* **1998**, *102*, 489.
(35) Lebedeva, N. P.; Koper, M. T. M.; Feliu, J. M.; van Santen, R. A. *J. Electroanal. Chem.* **2002**, *524*−*525*, 242.
(36) Funtikov, A. M.; Stimming, U.; Vogel, R. *J. Electroanal. Chem.* **1997**, *428*, 147.

(37) Koper, M. T. M.; Lukkien, J. J. *J. Electroanal. Chem.* **2000**, *485*, 161.
(38) Clavilier, J.; El Achi, K.; Petit, M.; Rodes, A.; Zamakhchari, M. A. *J. Electroanal. Chem.* **1990**, *295*, 333.
(39) Koper, M. T. M.; Lukkien, J. J.; Lebedeva, N. P.; Feliu, J. M.; van Santen, R. A. *Surf. Sci.* **2001**, *478*, L339.
(40) Marković, N. M.; Marinković, N. S.; Adzic, R. R. *J. Electroanal. Chem.* **1988**, *241*, 309.
(41) Marković, N. M.; Marinković, N. S.; Adzic, R. R. *J. Electroanal. Chem.* **1991**, *314*, 289.
(42) Clavilier, J.; El Achi, K.; Rodes, A. *J. Electroanal. Chem.* **1989**, *272*, 253.
(43) Clavilier, J.; Rodes, A. *J. Electroanal. Chem.* **1993**, *348*, 247.
(44) Gasteiger, H. A.; Marković, N.; Ross, P. N., Jr.; Cairns, E. J. *J. Phys. Chem.* **1994**, *98*, 617.
(45) Saravanan, C.; Koper, M. T. M.; Marković, N. M.; Head-Gordon, M.; Ross, P. N. *Phys. Chem. Chem. Phys.* **2002**, *4*, 2660.
(46) Lebedeva, N. P.; Rodes, A.; Feliu, J. M.; Koper, M. T. M.; van Santen, R. A. *J. Phys. Chem. B* **2002**, *106*, 9863.
(47) Bard, A. J.; Faulkner, L. R. *Electrochemical Methods: Fundamentals and Applications*; Wiley: New York, 2001.
(48) Wang, H.; Baltruschat, H. *Proc. Electrochem. Soc.* **2001**, *2001*−*4*, 50.